



# Photo-polymerisation of composite resins measured by micro-Raman spectroscopy

Alberto De Santis<sup>a,\*</sup>, Mario Baldi<sup>b</sup>

<sup>a</sup>Facoltà di Agraria, DiSA and INFM, Università della Tuscia, Via S.C. De Lellis, 01100 Viterbo, Italy

<sup>b</sup>Dipartimento di Scienze Chirurgiche, Clinica Odontostomatologica, Dir. Prof. Mario Giannoni, Università dell'Aquila, via Vetoio, 67100 L'Aquila, Italy

Received 8 September 2003; received in revised form 6 March 2004; accepted 23 March 2004

## Abstract

The micro-Raman spectroscopy was used for measuring the photo-polymerisation of composite resins. The elevated spatial resolution of the technique revealed surface non-homogeneities via the intensity variations of a strong band at  $1400\text{ cm}^{-1}$  and the presence of weak bands around the C=C and C=O stretching frequencies. Values of the degree of monomer conversion (DC) were determined for samples of Z100 commercial composite irradiated with different wavelength laser beams. Two methods were used for obtaining DC values. The first one exploits band decompositions in the spectral region of interest around  $1608$  and  $1637\text{ cm}^{-1}$ . The non-uniqueness of the decomposition introduces relevant uncertainties, which are amplified by unwanted weak bands. An alternative method, avoiding any fit procedure and exploiting the band shape conservation under irradiation, was found producing more reliable results. The  $632\text{ nm}$  line of the He–Ne laser was used as an exciting source. The measurements of the DC versus time are reported for three different wavelengths of the irradiation light. Preliminary studies of the C=O stretching bands are also reported. Their intensities decrease under irradiation and there are indications of a behaviour similar to that of the C=C aliphatic band.

© 2004 Elsevier Ltd. All rights reserved.

**Keywords:** Polymer composite materials; Micro-Raman spectroscopy; Photo-polymerisation

## 1. Introduction

To determine the degree of conversion (DC) of C=C double bonds of the methacrylate group in resin samples, mechanical (dilatometric), calorimetric and spectroscopic techniques can be used [1]. In principle, the last method provides more reliable results. The dilatometric technique, for example, can produce systematic errors, since the double bond conversion still proceeds in the glass state when the glassy resin shrinkage is frozen. The spectroscopic methods provide the direct measurements of the DC value because specific vibrational bands can be used as internal standards. In the urethane dimethacrylate based resin, N–H and C=O vibrations of the urethane were chosen as the reference bands. In the bis-GMA based resins, one uses the carbon–carbon aromatic vibration at  $1608$  and  $1583\text{ cm}^{-1}$ , or, in some cases, the C=O bands at  $1715\text{ cm}^{-1}$  [2] or the band of a filling substance such as the quartz band at  $465\text{ cm}^{-1}$  [1].

The choice of the internal standard requires some caution; the use of the C=O band as a reference was criticised [1,3] because more than one band can be associated with the carbonyl group and their intensity varies as the polymerisation grows. By contrast, the methacrylate group is not influent upon the aromatic ring which is unaffected by the polymerisation processes; the use of the aromatic C=C bands as an internal standard is therefore suitable.

The bis-GMA is the basic monomer constituent of many restorative dental materials because the aromatic rings and the hydrogen bonds, formed by the hydroxyl groups [4], yield strong rigidity to the resin matrix. Unfortunately, they also produce strong viscosity that makes the pure bis-GMA of difficult use. The triethylene or polyethylene glycol dimethacrylate (TEGDMA or PEGDMA, respectively) are used as diluents [5] for increasing the fluidity and improving the clinical handling. In such a situation, the photo-polymerisation increases with the diluent percentage, ranging from 40% (pure bis-GMA) to about 75% (pure TEGDMA) [4]. The higher mobility of the TEGDMA, due to major flexibility and minor molecular weight, seems to be

\* Corresponding author. Tel.: +39-0761357356; fax: +39-0761357327.  
E-mail address: [desantis@unitus.it](mailto:desantis@unitus.it) (A. De Santis).

responsible for its higher polymerisation and for the conversion of double bonds after the cure [6,7]. The modern commercial resins, however, are mostly formed by fillers whose concentration is kept high (about 80% by weight). In general, the filler consists of particles of amorphous silica whose size ranges in preponderance from submicron to 7  $\mu\text{m}$ . They are coated with silane couplers, which can copolymerise with the matrix resin. The particles of silica contribute to the C=C photo-conversion via a multiple light scattering mechanism [7]. In some commercial samples, pre-polymerised resin fillers are used. In such cases, the Fourier transform infra red (FTIR) spectroscopic technique was found to give systematic errors; the DC from FTIR was 30% lower than that obtained from differential thermal analysis (DTA) [8]. The effect was due to the inclusion of unreacted C=C in the filler which are 'seen' by FTIR and not by DTA.

This overview indicates that no standard method is available and, depending on the specific sample and/or instrumental apparatus, one has to search the best procedure and accuracy. In this work, we report the results of applying the micro-Raman spectroscopy to the DC measurement of the Z100 commercial resin. This technique is particularly useful for studying a sample surface or a two samples interface, as the resin–dentin interface [9]; the easy acquisition introduced by the CCD devices, the working in line-scanning mode and the possibility of focusing up to the diameter of 1  $\mu\text{m}$  make the technique very convenient. In view of systematic studies of the efficiency of different lamps and of the penetration of different composites in dental channels, we search for a reliable procedure for obtaining DC values from the irradiated commercial resins.

## 2. Materials and methods

### 2.1. Specimens

The commercial composite employed in this work was Z100 of 3M, Minneapolis, MN, USA. Its major components are bis-GMA (9%), TEGDMA (9%) and silane-treated micro-particles (80%), the percentages being by weight. The micro-particles consist of amorphous silica ( $\text{SiO}_2$ ) and micro-crystals of zirconia ( $\text{ZrO}_2$ ). The resin was placed in a holder ring of internal diameter of about 0.5 cm and thickness of 2 mm. The top surface was exposed to the radiation of a commercial lamp for dental restoring. To test the efficiency of light penetration, Raman spectra were recorded from points of both the sample surfaces and the conversion degrees computed.

### 2.2. Micro-Raman

The experimental apparatus was a Labram–Dilor spectrometer (Jobin–Yvon) with a 1800 g/mm grating and coupled with a high stability microscope; the objectives

50 $\times$  or 100 $\times$ , usually used, collect the signal in back scattering geometry from a focal spot area of few  $\mu\text{m}$  in diameter. A notch filter (model super notch plus) used as dichroic mirror, reflects the light on the sample and transmits the back-scattered Raman signal. The detector was a Peltier cooled CCD of 1024  $\times$  256 pixels and, with the 632.8 nm excitation wavelength (provided by the internal He–Ne laser), a single Raman spectrum was detected over the frequency range 1000–1900  $\text{cm}^{-1}$ . The spectral resolution was of about 5  $\text{cm}^{-1}$ , and usually, a photon counting time of 60 s ensured sufficiently good statistics. Other three laser lines, each one requiring a specific notch filter, at the wavelengths 514.5 and 488.0 nm (Ar laser) and 451 nm (He–Cd) were available as exciting beams. A check of the DC conversion versus wavelength was performed (see Fig. 9) and the use of the exciting wavelength of 632.8 nm was chosen for its complete inefficiency in composite photo-conversion. To our knowledge, no experiment exploiting a laser probe at the visible wavelengths has been recently performed on photo-polymerising composites. The micro-Raman spectroscopy, which exploits the 514.5 nm line, was successfully applied to the resin–dentin interface studies of polymerised materials [9]. An attempt of obtaining Raman spectra of Z100 composite was unsuccessful owing to an excess of fluorescence [10]. The use of the exciting wavelength of 632.8 nm, for which the response of the LabRam spectrometer is optimised, represents a good compromise between (a) the fluorescence minimisation (fluorescence decreases as the wavelength increases), (b) a sufficient efficiency of the Raman cross-section (which decreases by  $1/\lambda^4$  as  $\lambda$  increases) and (c) the need of ensuring the complete absence of photo-conversion.

### 2.3. Vibrational lines assignments

From the literature, one knows the frequency of vibrational lines for the basic components of commercial resins, i.e. for bis-GMA and TEGDMA (or PEGDMA) [3,5]. Vibrational line assignments of the Z100 composite were

Table 1  
Vibrational line assignments from Refs. [1,3,10,11,16]

Frequency ( $\text{cm}^{-1}$ )	Band assignments
465	Quartz filler
500	Zirconium filler
806	Si–O–Si bending
1100	Si–O stretching
1050–1300	Aliphatic C–O stretching
1404	>C=CH <sub>2</sub> bending
1457, 1513, 1558	Skeletal vibrations of the benzene ring
1508, 1578	C=C aromatic stretching
1608	C=C aromatic stretching
1638	C=C aliphatic stretching
1702	C=O hydrogen bonded stretching
1718	C=O free stretching

obtained by infrared spectra [10]. They are listed in Table 1. The bands at 1608 and 1583  $\text{cm}^{-1}$  [11] are associated with the aromatic C=C stretching vibrations and can be used as internal standards. Another band, centred around 1576  $\text{cm}^{-1}$  (see Fig. 4) and as weak as the 1583  $\text{cm}^{-1}$  band, is insensitive to irradiation and can be used as an internal standard. It is probably attributable to aromatic C=C stretching vibrations or to the more complex vibrations referred to as the skeletal vibrations of the benzene ring. The band at 1638  $\text{cm}^{-1}$  is due to the aliphatic C=C stretching vibrations and its intensity decreases as the polymer matrix grows. Usually, the 1608 and 1638  $\text{cm}^{-1}$  bands are used to evaluate DC values (see Section 3.2). The bands between 1700 and 1730  $\text{cm}^{-1}$  are due to the C=O stretching [1–3]. A first band at about 1700  $\text{cm}^{-1}$  is attributed to hydrogen bonded carbonyl groups, since its intensity decreases linearly with the C=C double bonds conversion. The second one, at 1717  $\text{cm}^{-1}$ , is due to free vibrations of carbonyl groups and it is less sensitive to the C=C conversion. In the case of pure bis-GMA Raman spectra, the photo-polymerisation affects also the band at about 1400  $\text{cm}^{-1}$ . This band has been attributed to modes of C=CH<sub>2</sub> [1]. At low frequencies, one has the bands due to the fillers, such as silica and zirconia, while at the higher frequencies (beyond 2000  $\text{cm}^{-1}$ ) the stretching bands of C–H and O–H are present. These frequency ranges are not investigated in the present work.

### 3. Results and discussions

#### 3.1. Data treatment and band assignments

In Fig. 1, the spectrum of the non-polymerised Z100 composite is shown. It was obtained by using the 632.8 nm

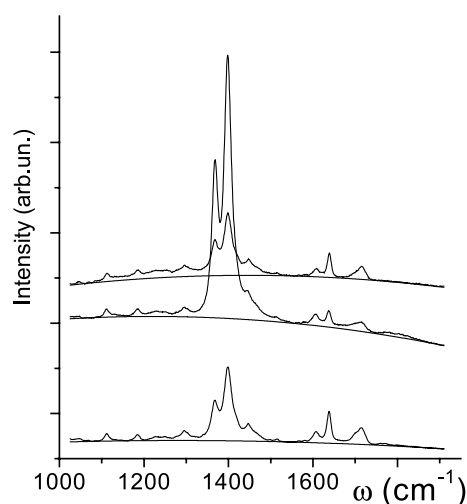


Fig. 1. Raman spectra of the Z100 composite and parabolic interpolations of the background. The spectra are from different surface points and for different irradiation times. They show, in particular, the difference in the intensity of the band around 1400  $\text{cm}^{-1}$ .

excitation wavelength. The Raman signal is superimposed to a fluorescence broad band whose intensity decreases in time reaching a stable intensity level in few minutes. The fluorescence signal is subtracted by using a polynomial interpolation given by the lowest degree polynomial matching few selected minimum points of the spectrum (see Fig. 1); in general, the second-degree was sufficient. The spectra of Fig. 1 refer to different points of the same sample (one of them after the sample irradiation) and show differences in both the level and shape of the fluorescence background. Pure Raman spectra, obtained after the baseline subtraction, are shown in Fig. 2. All the main bands, reported in Table 1, are present. But the Raman bands around 1400  $\text{cm}^{-1}$ , attributed to the C=CH<sub>2</sub> modes [3], differ from the corresponding bands of the bis-GMA spectra. Moreover, in bis-GMA, such bands strongly decrease with the polymerisation time. In the case of Z100 composite, we found that they can vary from one surface point to another and no polymerisation decrease is observed. The spectra of Fig. 2 were chosen to show the strong difference one can obtain. The band at 1400  $\text{cm}^{-1}$  of the irradiated sample shows the strongest intensity, meaning that the associated vibrations are independent of the aliphatic C=C motions of bis-GMA. The enhancements of the band intensity between 1350 and 1450  $\text{cm}^{-1}$ , could be due to the symmetric and anti-symmetric bending of the CH<sub>2</sub> and CH<sub>3</sub> groups [12] due to the silanes, used as coupling agents between the fillers and the organic matrix. This is because the very strong intensity at 1400  $\text{cm}^{-1}$  is obtained rarely. Normally, a moderate intensity variation is detected by varying the surface points, one point corresponding to the laser spot area (few  $\mu\text{m}^2$ ). At this detail level, the average number of filling particles fluctuates significantly, yielding fluctuations of the Raman signal too.

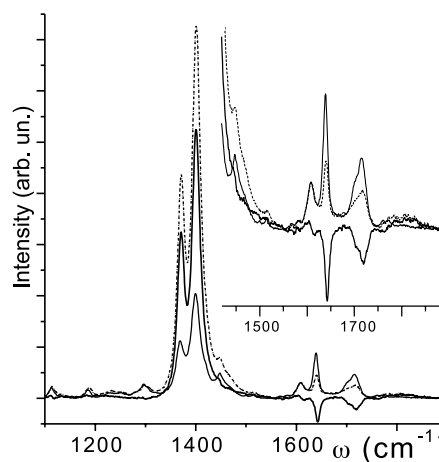


Fig. 2. Raman spectra from two different surface points of the same sample, before (thin solid line) and after (dashed line) irradiation. The intensities are arbitrarily scaled to overlap around 1608  $\text{cm}^{-1}$ . The inset magnifies the frequency zones of the C=C and C=O stretchings. Also shown is the difference spectrum (thick solid line) showing the resulting upside-down bands of the aliphatic C=C bond (1637  $\text{cm}^{-1}$ ) and carbonyl C=O bond (1710  $\text{cm}^{-1}$ ).

In some infrequent cases, it is possible focusing near a single large diameter filler (the fillers can reach the diameter of 7  $\mu\text{m}$ ) and capturing strong Raman scattering from the bridging silanes.

For our purposes, however, it is important understanding how much the surface non-homogeneities influence the DC measurements. Fig. 2 shows the difference between polymerised and non-polymerised spectra normalised to the aromatic C=C vibration band intensity at 1608  $\text{cm}^{-1}$ . As is seen, the band at 1450  $\text{cm}^{-1}$  disappears and only those at 1370 and 1400  $\text{cm}^{-1}$  survive. Therefore, the 1450  $\text{cm}^{-1}$  band can be attributed to the network vibrations of organic compounds, as the weak bands between 1000 and 1400  $\text{cm}^{-1}$  [12] which are practically unaffected by the irradiation. Around the frequency of 1800  $\text{cm}^{-1}$ , one can see some bands in the difference spectrum. They are present in the polymerised spectrum and absent in the non-polymerised one; consequently, they are likely due to differences in the surface composition rather than due to photo-polymerisation effects.

To stress the point-to-point differences on the samples surfaces, we recorded two after-irradiation spectra obtained from different surface points of the same sample. They are shown in Fig. 3. Their difference is shown separately in the left inset and by the bold curves appearing in both the main picture and the right inset. The presence of bands at about 1800  $\text{cm}^{-1}$  and of other weak bands just around the C=C stretching frequency is evident. Together with the bands at 1370 and 1400  $\text{cm}^{-1}$ , they are attributable to the sample surface non-homogeneity and, for the discussion performed above, likely due to the fillers.

In summary, it has been shown that: (a) owing to the considerable size the filler reaches, the sample appears non-homogeneous in the micro-Raman scattering area, (b) two bands at about 1370 and 1400  $\text{cm}^{-1}$  characterise the non-

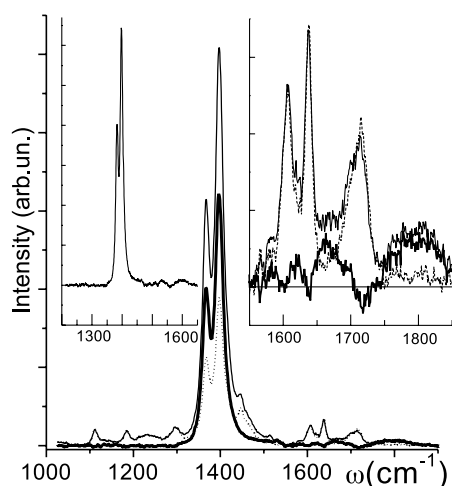


Fig. 3. After irradiation Raman spectra of the same sample recorded from two different surface points (thin solid and dotted lines) and their difference (thick solid line). The left side inset shows the total difference spectrum and the right side one is the magnification of the main picture, around the C=C and C=O bonds.

homogeneity. Their assignment is uncertain; the bridging silanes could be involved and (c) other weak bands join to the two principal ones mentioned above. They appear in the frequency zone of the C=C and C=O stretching and could perturb the DC measurement significantly.

### 3.2. The evaluation of the degree of conversion

The DC of the composites is defined by:

$$\text{DC} = 1 - (I_{1637}^i/I_{1608}^i)/(I_{1637}^n/I_{1608}^n) \quad (1)$$

where  $I^i$  and  $I^n$  stand for the band integrated intensities of the irradiated and non-irradiated samples, respectively. This way of computing DC is hereafter referred to as the integrated intensity ratio (IIR). To obtain the intensity of each band, one needs performing the band decomposition (usually through a best fit procedure) and calculating the area of the fitting curves. The first difficulty of this procedure consists in the functional form one uses. Generally, one chooses a Gaussian, a Lorentzian or a mixed form of the two functions. Assignments of the spectral shapes have been performed in Ref. [1] for the carbonyl bands that result purely Gaussian at 1715  $\text{cm}^{-1}$  and mixed 1/1 Lorentzian/Gaussian at 1700  $\text{cm}^{-1}$ . Fig. 4 shows an example of band decomposition obtained by applying a standard  $\chi^2$  minimisation procedure [13]. The Lorentzian/Gaussian parameter (ranging from 0 to 1) was free for the bands at 1608, 1637 and 1700  $\text{cm}^{-1}$ . The other ones at 1567, 1580 and 1715  $\text{cm}^{-1}$  was fixed to the Gaussian shape [3]. The band shapes at 1700 and 1650  $\text{cm}^{-1}$  turn out 100% Lorentzian, instead of 50% as in Ref. [3]. This result is influenced by the presence of weak spurious bands (see Figs. 2 and 3 and Section 3.4). The C=C 1637  $\text{cm}^{-1}$  and C=O 1700  $\text{cm}^{-1}$  bands are induced to have a strong Lorentzian shape to reproduce the background that the weak bands around 1650  $\text{cm}^{-1}$  produce. Consequently,

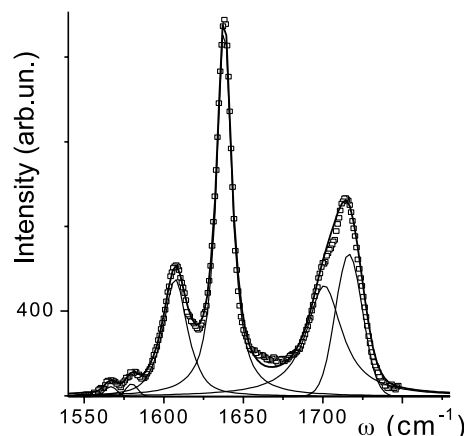


Fig. 4. Non-polymerised Z100 Raman spectrum and the best fitting curves (thin underlying lines) at the frequencies of 1567  $\text{cm}^{-1}$  (100% Gaussian), 1580  $\text{cm}^{-1}$  (100% Gaussian), 1608  $\text{cm}^{-1}$  (70% Lorentzian), 1638  $\text{cm}^{-1}$  (100% Lorentzian), 1701  $\text{cm}^{-1}$  (100% Lorentzian), 1716  $\text{cm}^{-1}$  (100% Gaussian). The thick line is the sum of the component curves.

they result 100% Lorentzian. A similar effect is produced by an insufficient baseline subtraction. A residual baseline can bring the fit to favour the Lorentzian part of the line shape in order to match the base line with far wings. These effects can yield significant variations on the band area calculation and on the DC value. An example of the data fluctuations obtained with this method is shown in Fig. 9 of Section 3.3.

A different approach, which avoids the use of area calculations and produces more reproducible DC data, is proposed. The basic idea is that the band frequency and intensity are conserved during the irradiation (band shape conservation). One can define a frequency dependent ratio,  $DC(\omega)$  (a DC dependent on the frequency  $\omega$ , as shown in Appendix A), as

$$DC(\omega) = [I^n(\omega) - I^s(\omega)]/I^n(\omega) = D(\omega)/I^n(\omega) \quad (2)$$

where  $I^s$  stands for the spectral intensity of the irradiated sample scaled for matching the internal standard intensity to that of the non-irradiated one (Eq. (A1) of Appendix A) and  $D(\omega)$  stands for the spectral difference between  $I^s$  and  $I^n$  spectra. If a given band shape is conserved,  $DC(\omega)$  becomes frequency independent and, for the  $1637 \text{ cm}^{-1}$  band, it yields the best estimate of DC as

$$DC = 1 - I_{1637}^s(\omega_p)/I_{1637}^n(\omega_p) \quad (3)$$

where  $\omega_p$  is the peak frequency. The details are reported in Appendix A. One has to check the assumptions leading to Eq. (3) (or to Eq. (A7) of Appendix A) as follows: the difference spectrum  $D(\omega)$  and its ratio to  $I^n(\omega)$  are computed. In the frequency range where the intensities of the  $I_{1637}^n(\omega)$  and  $I_{1637}^s(\omega)$  bands are dominant, the  $DC(\omega)$  shape should be flat or slightly bumped around the peak frequency. If so, the reliability of Eq. (2) (and of Eqs. (A4) and (A7) of Appendix A) is assumed, otherwise it is rejected. Obviously, the rejection should follow a critical study of spurious bands and unwanted residual background.

Figs. 5 and 6 show the results of this procedure, hereafter referred to as the single frequency intensity ratio (SFIR). In Fig. 5, the  $DC(\omega)$  is compared with the difference,  $D(\omega)$ , and with the non-polymerised spectra  $I^n(\omega)$ , both suitably scaled and shifted. The vertical bars indicate the zones where a

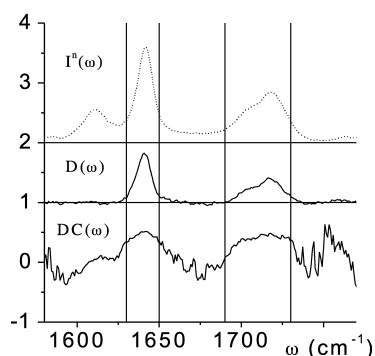


Fig. 5. The non-irradiated spectrum  $I^n(\omega)$  (dashed line), the difference spectrum  $D(\omega)$  (non-polymerised minus polymerised) (thin solid line), and the ratio of Eq. (A6) yielding  $DC(\omega)$  (thick solid line).

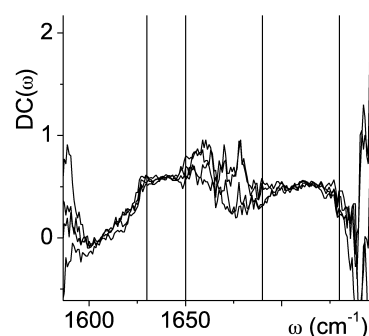


Fig. 6. Degree of conversion versus frequency computed from Eq. (A6) and the spectrum obtained from four different points of the same irradiated sample.

nearly flat behaviour could be present, namely  $1630 < \omega < 1650 \text{ cm}^{-1}$  and  $1690 < \omega < 1730 \text{ cm}^{-1}$ . This last zone refers to the carbonyl bands and will be discussed later. As is seen, near the edges of the first zone,  $DC(\omega)$  tends to decrease. The effect is essentially due to the presence of the spurious bands whose influence grows as one moves from the peak to the wings of the  $1637 \text{ cm}^{-1}$  band. As already shown in Fig. 3, such bands are related to the presence of the  $1400 \text{ cm}^{-1}$  band and can differ from one spectrum to another, if the spectra are taken from different surface points. Fig. 6 shows the case of surface points of the same sample less disturbed by spurious effects. Two of them belong to the bottom surface. The flat trends between  $1630$  and  $1650 \text{ cm}^{-1}$ , and between  $1690$  and  $1730 \text{ cm}^{-1}$  are very well defined. Outside, there are strong oscillations due to the background. For example, between  $1650$  and  $1690 \text{ cm}^{-1}$ , i.e. in the frequency zone delimited by the C=C and C=O stretching, no vibrational bands should be present following the assignments of the literature (Table 1). But the more or less intense spurious bands of Fig. 3 or the presence of a residual background can affect the ratio  $DC(\omega)$  of Eq. (A6) yielding the different average levels of  $DC(\omega)$  shown in Fig. 6. The same figure also shows that such differences do not alter significantly the  $DC(\omega)$  in the C=C stretching zone.

These results lead to following conclusions:

1. the band shape is conserved and all the implications of Eqs. (2) and (A1)–(A7) hold good. The conversion degree, DC, can be obtained from the  $DC(\omega)$  values around the peak frequency  $\omega_p = 1637 \text{ cm}^{-1}$ . Notwithstanding background and/or spurious bands, in the frequency interval determined by the half width at the half maximum of the difference peak, the influence of such unwanted signals is negligible. The DC value can be conveniently chosen as  $DC(\omega_p)$ .
2. Two plots of  $DC(\omega)$ , shown in Fig. 6, refer to points on the bottom surface. Since the sample was irradiated on the top, the complete polymerisation at the bottom indicates complete light penetration in the Z100 composite. Consequently, the surface results, obtained by the micro-Raman spectroscopy, hold for the bulk too.

### 3.3. Polymerisation versus wavelength

The degree of double bond conversion depends on the irradiation dose one uses [15]. However, there is a strong wavelength effect enhanced around the blue frequencies. To obtain DC measurements by the Raman spectroscopy, it is necessary to check the complete independence of the polymerisation mechanism on the monochromatic radiation used as probe. To prevent spectral variations due to different surface points, we realised the experimental condition shown in Fig. 7. An objective with long work distance (2.5 cm) and magnification of  $20\times$  was used and the probe laser beam ( $\lambda = 632.8$  nm) was focused on the same surface point. The sample was exposed to the irradiation beam for a chosen time interval and soon after the measurement was performed. In general, a counting time of 120 s was used. The irradiation, at the 514.5 and 488.8 nm (Ar laser) and 451 nm (He–Cd laser) wavelengths, was obtained from available external laser sources usually exploited as external exciting beams, alternative to the He–Ne laser placed inside the spectrometer. The laser beam intensity was adjusted to have about  $350$  mW/cm<sup>2</sup>, as is the case of lamps used in dental restoring. To obtain the DC values, both the methods of the IIR (the IIR method of Eq. (1)) and of the SFIR were used. The results are shown in Figs. 8 and 9. As is evident SFIR yields more reproducible results than IIR. Note also that the 488 and 451 nm wavelengths yield the same DC values. The asymptotic trend agrees with previous results [4, 14]. A very low degree of polymerisation seems to be induced by the green line at 514.5 nm. To assign characteristic times, the following function was fitted to the experimental data

$$y(t) = a_1(1 - e^{-t/\tau_1}) + a_2(1 - e^{-t/\tau_2}) \quad (4)$$

The two relaxation times are necessary to fit the data of samples irradiated with blue and violet laser lines. It resulted in  $a_1 = 0.31$ ,  $\tau_1 = 1.3$  s and  $a_2 = 0.13$ ,  $\tau_2 = 29$  s. There are two different processes, the first one that raises rapidly the DC value by about 75% of the final value. The remaining 25% is achieved slowly. The kinetics of the polymerisation of a one-component resin is quite complex, being made of autoacceleration (or gel effect), diffusion limited processes and a maximum DC, which can be significantly less than unity. Very slow polymerisation was also observed in the post-irradiation time [6], an effect not

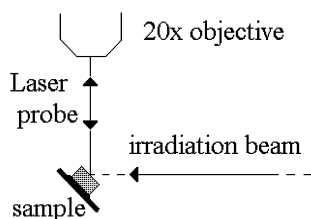


Fig. 7. Sketch of the geometry used for measuring the time dependence of the degree of conversion. The horizontal beam was in turn at the laser wavelengths of 451, 488.8 and 514 nm.

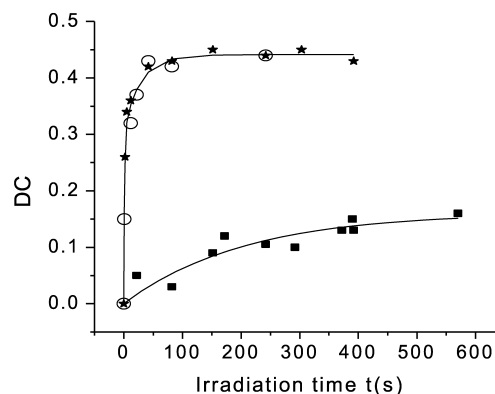


Fig. 8. The degree of conversion, DC, computed with the single frequency intensity ratio (SFIR) method, versus the irradiation time and for different wavelengths: 451 nm (open circle), 488.8 nm (black star) and 514.5 nm (black square). The solid lines are the interpolation curves obtained from the best fit of Eq. (4).

investigated in the present work. Moreover, pure TEGDMA resin polymerises much more slowly than pure bis-GMA ( $\tau \sim 20$  s against  $\tau \sim 1$  s), but reaches a higher conversion degree (75.7% against 39.0%) [4]. Z100 contains equal quantities of bis-GMA and TEGDMA; consequently, the fast and slow relaxation times are likely due to the different polymerisation rates of bis-GMA and TEGDMA, respectively. For the irradiation with the green laser line, Eq. (4) reduces to a single exponential with  $a_1 = 0.16$ ,  $\tau_1 = 204$  s. The related DC data are affected by strong uncertainties mainly at short times. Moreover, a slightly less transparent Z100 sample (the B3 type instead of the B2 one) resulted practically being insensitive to the irradiation. One concludes that the photo-conversion due to the green radiation is nearly vanishing. The effects of the red line, used as probe, were investigated by comparing spectra recorded soon after few seconds and after hours of exposition. No difference was recorded. Since the characteristic times of the photo-polymerisation are not very long, this measurement does not provide evidence for the absence of polymerisation. This is also because an unwanted

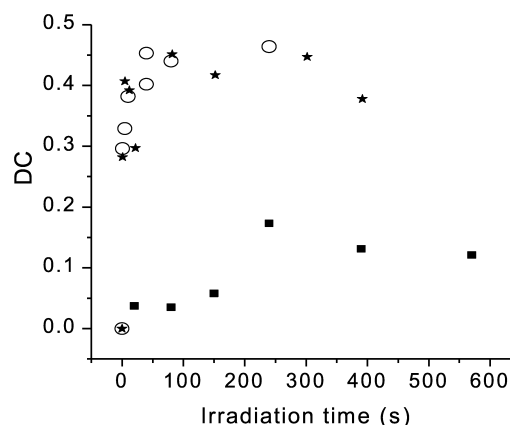


Fig. 9. Degree of conversion, DC, computed with the integrated intensity ratio (IIR) method, versus wavelength: 451 nm (open circle), 488.8 nm (black star) and 514.5 nm (black square).

exposure is performed when, before any measurement, one irradiates the sample for partially quenching the fluorescence. The nearly vanishing effects of the green laser line, with respect to the violet one, ensure that no polymerisation occurs for exposition to the red radiation.

### 3.4. The C=O stretching frequency region

The C=O stretching frequency zone is indirectly involved in the polymerisation process. It was found that the Raman spectrum of pure bis-GMA shows two bands at 1700 and 1718  $\text{cm}^{-1}$  [3], attributed to the stretching of hydrogen bonded and free carbonyl groups, respectively, the hydrogen bonds occurring between the carbonyl and hydroxyl groups. It was found that, during the polymerisation, the intensity of the band at 1700  $\text{cm}^{-1}$  decreases linearly with the monomer conversion, while that at 1720  $\text{cm}^{-1}$  is practically constant. These effects were explained in terms of strength alterations of hydrogen bonds. One can define a degree of apparent conversion (DAC) as follows

$$\text{DAC} = 1 - (I_{\text{C=O}}^i/I_{1608}^i)/(I_{\text{C=O}}^n/I_{1608}^n) \quad (5)$$

where  $I_{\text{C=O}}$  stands for the total intensity of a carbonyl band. The frequency dependent form,  $\text{DAC}(\omega)$ , is given by Eq. (2). If the band shape is conserved, one can exploit the results of Section 3.2 and compute the DAC from

$$\text{DAC} = 1 - I^s(\omega_{\text{C=O}})/I^n(\omega_{\text{C=O}}) \quad (6)$$

where  $\omega_{\text{C=O}}$  is the frequency of a suitable point in the C=O frequency zone. The results of Figs. 5 and 6 show nearly flat trends around the peak frequencies of the bands at 1700 and 1720  $\text{cm}^{-1}$  (see the band decomposition of Fig. 4). This indicates an effect of photo-conversion and confirms that the carbonyl bands cannot be used as internal standard for Raman spectroscopic studies, in agreement with Ref. [3]. The flat trends also suggest an effect of band shape conservation and the possibility of using Eq. (6) for determining the apparent DC. Since some causes of the apparent C=O conversion (e.g. frequency shifts) would involve band shape variation, we will devote an 'ad hoc' careful analysis to the C=O band intensity variation with the irradiation exposure time.

## 4. Final conclusions

It has been shown that the micro-Raman spectroscopy provides accurate quantitative information on the degree of polymerisation of composite resins. The technique is able to detect differences in the Raman spectra obtained from different surface points owing to its high spatial resolution. In the case of Z100 commercial composite, the intensity of a band at 1400  $\text{cm}^{-1}$  has been found strongly dependent on the surface points. Its presence is accompanied by minor bands which affect the C=C frequency zone. This and the unknown C=C band shapes can influence the DC evaluation

performed via the band decomposition and integration. We have shown that the band shape of the aliphatic C=C double bond is conserved under irradiation and an alternative way of measuring DC is proposed. Accurate measurements of the DC dependence on the exposure to monochromatic radiations are obtained for various wavelengths. In the C=O frequency zone,  $\text{DC}(\omega)$  results nearly constant. This indicates the band shape conservation. In this case, the comparison of the SFIR and IIR results is particularly interesting and is planned as a future investigation. Finally, the possibility of applying a non-destructive micro-Raman technique allows an easy determination of some effects of the photo-conversion, such as the effects of the light penetration in part investigated in this work.

## Acknowledgements

The research was supported by grants of the agencies INFN and MIUR. The encouragements of Prof. G. Signorelli and the support of Prof. V. Mazzacurati, as Sect. C—INFN director, received in the near past, are gratefully acknowledged.

## Appendix A

We report the details of the procedure used to obtain the DC from a SFIR method. The procedure is composed of the following steps:

(a) After the background fluorescence is subtracted, one searches for a scaling factor  $\alpha$  which brings the 1608  $\text{cm}^{-1}$  band (internal standard) of irradiated and non-irradiated samples to overlap, i.e.

$$I_{1608}^n(\omega) = \alpha I_{1608}^i(\omega) \quad (\text{A1})$$

If the experimental conditions were exactly the same while detecting the spectra of irradiated and non-irradiated sample, it would be  $\alpha = 1$ . The results of scaling are shown in Figs. 2 and 3. As one can see, the overlap of the bands at 1608  $\text{cm}^{-1}$  is very good. This supports the use of such a band as a standard. Then, Eq. (1) of the main text can be written as

$$\text{DC} = 1 - (\alpha I_{1637}^i/\alpha I_{1608}^i)/(I_{1637}^n/I_{1608}^n) \quad (\text{A2})$$

From Eq. (A1) it follows

$$\text{DC} = 1 - (\alpha I_{1637}^i/I_{1637}^n) = 1 - (I_{1637}^s/I_{1637}^n) \quad (\text{A3})$$

where  $I_{1637}^s = \alpha I_{1637}^i$  indicates the integrated band intensity of the irradiated sample scaled for matching the internal standard bands, as in Eq. (A1).

(b) One hypothesises that

$$I_{1637}^s(\omega) = \beta I_{1637}^n(\omega) \quad (\text{A4})$$

where  $0 \leq \beta \leq 1$  is a frequency independent factor. Eq.

(A4) implies that the irradiation produces intensity variation but conserves the spectral shape of the band at  $1637\text{ cm}^{-1}$ . This is a reasonable assumption since the remaining pendant C=C aliphatic double bonds of the irradiated sample belong to the same monomer structures of the pre-irradiated one; so, a band shape variation could arise only from a strong variation of the local Lorentz field due to the medium which surrounds the C=C bond. The polymerisation of the Z100 composite is expected producing no significant change. Then, Eq. (A3) becomes

$$DC = \int [I_{1637}^n(\omega) - I_{1637}^s(\omega)]d\omega / \int I_{1637}^n(\omega)d\omega = 1 - \beta \quad (\text{A5})$$

If the frequency dependent DC is defined as in Eq. (2), i.e.

$$DC(\omega) = [I^n(\omega) - I^s(\omega)]/I^n(\omega) = 1 - I^s(\omega)/I^n(\omega) \quad (\text{A6})$$

for the aliphatic C=C bands at  $1637\text{ cm}^{-1}$ , by exploiting Eq. (A4) one has

$$DC(\omega) = [I_{1637}^n(\omega) - I_{1637}^s(\omega)]/I_{1637}^n(\omega) = DC = 1 - \beta \quad (\text{A7})$$

Eq. (A7) stresses that DC values could be, in principle, obtained from the band intensity at any spectral frequency. In practice, one has to consider the band overlap, the noise, the presence of spurious bands and the imperfect background subtraction. Fig. A1 shows the simulation of Eqs. (A6) and (A7) in the cases (I) of two Gaussian functions, standing for the C=C stretching bands, and (II) of these two functions plus a constant standing for spurious bands or a

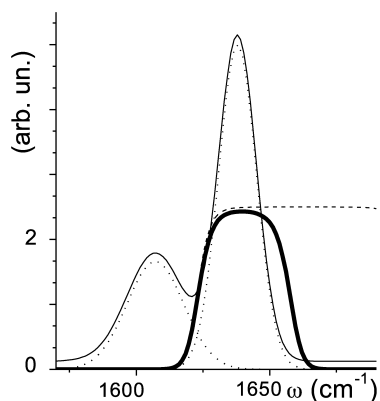


Fig. A1. Simulated band shape (arbitrary unit scale) in the C=C stretching frequency zone in two cases: (I) two Gaussian curves (•••) without background; the resulting  $DC(\omega)$  of Eq. (A6) is represented by the dashed curve (- - -). (II) The same two Gaussian bands plus a constant background of 0.025, yielding the sum spectrum represented by the thin solid line (—); the bold solid line (—) stands for the resulting function  $DC(\omega)$  of Eq. (A6).

residual fluorescence background. The band at  $1608\text{ cm}^{-1}$  was set 50% larger and 30% weaker than the  $1637\text{ cm}^{-1}$  one. The results are: (a) the band overlap effects are negligible. Indeed, beyond the peak frequency  $\omega_p \cong 1637\text{ cm}^{-1}$ ,  $DC(\omega)$  is constant and equal to 0.5, the hypothesised  $\beta$  value and (b) the addition of a small background destroys the flat trend of  $D(\omega)$ , and it results in a bumped shape centred at about  $\omega_p$ . In this case,  $DC(\omega_p)$  is the best estimate of the DC since the disturbances have the minimum effect.

Finally, we note that small frequency shifts between the spectra of non-irradiated and irradiated samples could produce significant errors in the DC calculation. In the dispersion spectrometers, a shift source could be due to the gratings movement, owing to the backlash effect or the linearity variations induced by the temperature drift. If one uses the CCD detectors, it is therefore suitable to perform the measurements of the irradiated sample and soon after that of the non-irradiated one in the same fixed spectral range.

## References

- [1] Sandner B, Kammer S, Wartewig S. *Polymer* 1996;37(21):4705–12.
- [2] Oréface RL, Discacciati JAC, Neves AD, Mansur HS, Jansen WC. *Polym Test* 2003;22:77–81.
- [3] Kammer S, Albinsky K, Sandner B, Wartewig S. *Polymer* 1999;40:1131–7.
- [4] Sideridou I, Tserki V, Papanastasiou G. *Biomaterials* 2002;23:1819–29.
- [5] Karmaker AC, Dibenedetto AT, Goldberg AJ. *J Mater Sci Mater Med* 1997;8:369–74.
- [6] Tarumi H, Imazato S, Ehara A, Kato S, Ebi N, Ebisu S. *Dent Mater* 1999;15:238–42.
- [7] Kim S, Jang J. *Mater Charact Polym Test* 1996;15:559–71.
- [8] Imazato S, McCabe JF, Tarumi H, Ehara A, Ebisu S. *Dent Mater* 2001;17:178–83.
- [9] Van Meerbeek B, Mohrbacher H, Celis JP, Roos JR, Braem M, Lambrechts P, Vanherle G. *J Dent Res* 1993;72(10):1423–8.
- [10] Xu J, Butler IS, Gibson DFR, Stangel I. *Biomaterials* 1997;18(24):1653–7.
- [11] Stansbury JW, Dickens SH. *Dent Mater* 2001;17:71–9. See also the references therein.
- [12] Gnyba M, Keränen M, Kozanecki M, Bogdanowicz R, Kosmowski BB, Wroczyński P. *Opto-Electron Rev* 2002;10(2):137–43.
- [13] The employed minimisation routine was supplied with the Labram–Dilor spectrometer as part of the user software for spectra handling. The mixed Lorentzian–Gaussian band shape is given by  $f(x) = A \exp[-[(\omega - \omega_0)/\sigma]^2] + (1 - A)/[1 + 4[(\omega - \omega_0)/\sigma]^2]$ .
- [14] Park Y-J, Chae K-H, Rawls HR. *Dent Mater* 1999;15:120–7.
- [15] Halvorson RH, Erickson RL, Davidson CL. *Dent Mater* 2002;18:463–9.
- [16] Mueller HJ, Freeman D. *Mater Charact* 1995;35:113–26.